RID

REPORTE
Imagenológico Dentomaxilofacial

ISSN: 2791-1888. e-id: e20240302 Número 2 Volumen 3 Julio-Diciembre 2024

Sociedad Venezolana de
Radiología e Imagenología
Dentomaxilofacial

Rep Imagenol Dentomaxilofacial 2024 julio-diciembre; 3(2): 2024030202
e-ISSN: 2791-1888| 1 de 8
Disponible en: https://publicaciones.svrid.org.ve/index.php/rid
DOI: 10.60094/RID.20240302-38

REPORTE TÉCNICO

Improved odontoma diagnosis via enamel mask in cone beam computed tomography

Diagnóstico mejorado de odontoma complejo por medio de máscara de esmalte en tomografia computarizada de haz cónico

Antonione Santos Bezerra Pinto[1], Maria Ângela Arêa Leão Ferraz[2], Carlos Alberto Monteiro Falcão[3], Moara e Silva Conceição Pinto[4], Luana Leal Cosmo Cardoso[5*], André Luca Araujo de Sousa[5]

[1]Assistant Professor of Pathology and Histology. Instituto de Educação Superior do Vale do Parnaíba (FAHESP/IESVAP). Parnaíba-PI, Brasil. antonione.pinto@iesvap.edu.br ORCID: 0000-0002-6577-2816

[2]Professor of Endodontics. Universidade Estadual de Piauí. Brasil. angelaferraz@phb.uespi.br ORCID: 0000-0001-5660-0222

[3]Professor of Oral Radiology. Universidade Estadual de Piauí. Brasil. falcao@phb.uespi.br ORCID: 0000-0001-7787-0280

[4]Post Graduation in Endodontics and Periodontics. Universidade Estadual de Piauí. Brasil. moara.c@hotmail.com ORCID: 0000-0003-3518-3890

[5]Undergraduation in Dentistry. Universidade Estadual de Piauí. Brasil. luanalccardoso@outlook.com ORCID: 0009-0000-5238-8789; a.lucaaraujo10@gmail.com ORCID: 0000-0003-4876-9188

Academic editor: Dra. Ana Isabel Ortega.

RESUMEN

Objetivo: evaluar la efectividad del uso de la máscara de esmalte en el software InVesalius para detectar regiones hiperdensas en imágenes de tomografía computarizada de haz cónico (TCHC) de focos de esmalte en odontomas complejos. **Materiales y métodos:** se analizaron 25 escaneos TCHC de pacientes que se sometieron a cirugía y diagnóstico histopatológico de odontomas complejos utilizando el software InVesalius, donde se utilizó la segmentación para seleccionar los focos de esmalte en la lesión. Se realizó un análisis estadístico descriptivo de los datos para evaluar la dispersión de los mismos. **Resultados:** la técnica de segmentación de imágenes por umbral fue efectiva en la identificación de áreas de esmalte en lesiones odontogénicas. El uso de la máscara de esmalte permitió una mejor visualización de las áreas hiperdensas en las imágenes. Las pruebas estadísticas mostraron una distribución normal para las medias de las áreas (p = 0,13, media = 3,74, DE = 0.38) y el tamaño promedio de las lesiones (p = 0,02, media = 2,54, DE = 0,23). No hubo una relación significativa entre la media y el tamaño promedio (p = 0,67). **Conclusión:** el uso del software InVesalius asociado con la máscara de esmalte demostró ser una herramienta efectiva en la detección de regiones hiperdensas asociadas con odontomas complejos.

Palabras clave: Odontoma Complejo, tomografía computarizada de haz cónico, software (DeCS)

Como citar: Pinto ASB, Ferraz MAAL, Falcão CAM, Pinto MSC, Cardoso LLC, de Sousa ALA. Diagnóstico mejorado de odontoma complejo por medio de máscara de esmalte en tomografia computarizada de haz cónico. Rep Imagenol Dentomaxilofacial 2024;3(2):e2024030202

Recibido: 22/05/2024
Aceptado: 18/07/2024
Publicado: 30/07/2024

Sociedad Venezolana de Radiología e Imagenologia Dentomaxilofacial

Rep Imagenol Dentomaxilofacial 2024 julio-diciembre; 3(2): 2024030202
e-ISSN: 2791-1888| 2 de 8
Disponible en: https://publicaciones.svrid.org.ve/index.php/rid

TECHNICAL REPORT

ABSTRACT

Objective: to evaluate the effectiveness of using the enamel mask in InVesalius software to detect hyperdense regions in cone beam computed tomography (CBCT) images of enamel foci in complex odontomas. Materials and methods: 25 CBCT scans of patients who underwent surgery and histopathological diagnosis of complex odontomas were analyzed using the InVesalius software, where segmentation was used to select the enamel foci in the lesion. A descriptive statistical analysis of the data was performed to evaluate the data dispersion. Results: The threshold image segmentation technique was effective in identifying areas of enamel in odontogenic lesions. The use of the enamel mask allowed a better visualization of the hyperdense areas in the images. Statistical tests showed normal distribution for the means of the areas (p = 0.13, mean = 3.74, SD = 0.38) and average size of the lesions (p = 0.02, mean = 2.54, SD = 0.23). There was no significant relationship between mean and average size (p = 0.67). Conclusion: the use of the InVesalius software associated with the enamel mask proved to be an effective tool in the detection of hyperdense regions associated with complex odontomas.

Keywords: Complex Odontoma, cone-beam computed tomography, software (MeSH)

INTRODUCCTION

Cone beam computed tomography (CBCT) is a diagnostic imaging tool that is increasingly used in dentistry. It is able to provide accurate information about the anatomy of the tooth and adjacent tissues in three dimensions [1, 2]. With its growing popularity from this technique, new possibilities for the use of specific software for analysis and processing of these images also arise [3- 5]. *InVesalius* is a free and open source image processing software that allows the visualization and analysis of medical images in three dimensions, including CBCT images. It offers a variety of tools for image segmentation and manipulation, making it possible to identify different tissues and structures with high precision [6- 8]. In this context, the detection of hyperdense regions on CBCT images becomes an important challenge for dental diagnosis [9- 11]. These regions may indicate the presence of enamel lesions, which may be associated with a variety of dental pathologies. However, identifying these lesions is not always easy, especially in more complex cases [2,13]. Thus, the aim of this study is to evaluate the effectiveness of using the enamel mask in *InVesalius* to detect hyperdense regions in CBCT images of enamel foci in complex odontomas.

MATERIALS AND METHODS

The present study qualifies as quantitative in a cross-sectional way, based on the collection of tomographic files for analysis using specific software to satisfy the objective of the study.

The sample was census, all 25 patients with tomographic images suggestive of complex odontomas and with surgery performed for surgical treatment and histopathological diagnosis (Figure 1), observed from October 2022 to March 2023 were included. The observation period was chosen based on the availability of data and the timeframe required to collect and analyze the CBCT images. This period allowed for the inclusion of a sufficient number of cases

for robust statistical analysis and coincided with the timeframe during which patients underwent surgeries and histopathological diagnoses of complex odontomas. Those patients who showed signs of neoplasms, cysts or other lesions that could influence the identification of structures of interest, in addition to patients under 18 years of age, were excluded.

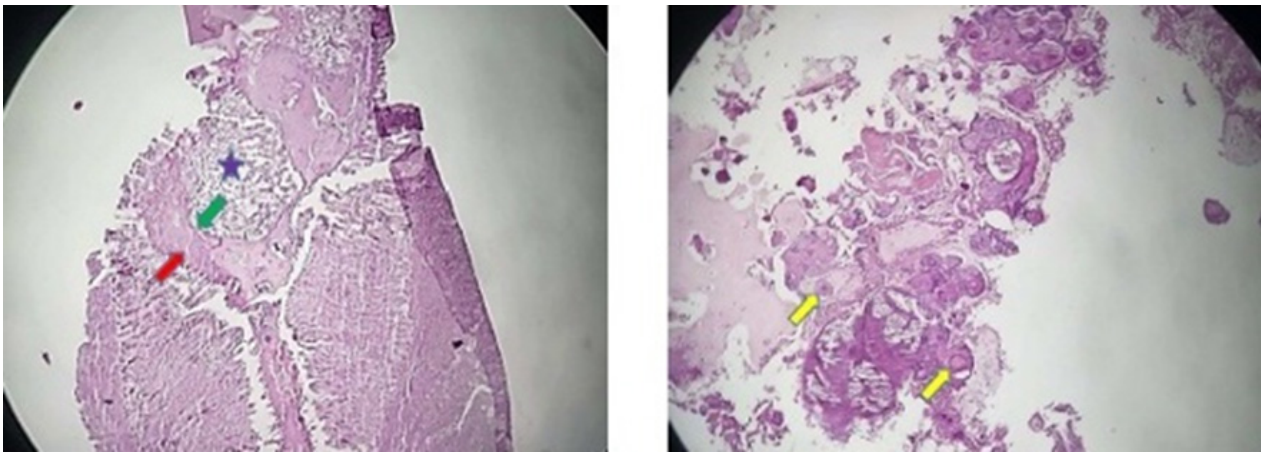

Figura 1. Figure 1. Histological sections of the odontoma stained with Hematoxylin-Eosin. Acellular matrix resembling fish scales indicating tooth enamel (red arrow) and row of columnar cells bordering this matrix in an ameloblast-like fashion (green arrow), followed by flattened cells that abruptly move apart maintaining intercellular bridges, loosely arranged, indicating the reticulum stellate of an enamel organ as in odontogenesis (star). Area showing basophilic mineralized material that forms spherical structures called cementicles, characterizing a formation of disorganized cementoid tissue (yellow arrows).

All procedures performed in studies involving human participants were in accordance with the ethical standards of the institutional research committee and with the 1964 Helsinki declaration and its comparable ethical standards (Ethics Committee Submission Code: 6.065.998). Informed consent was obtained from all individual participants included in the study for publication of their data.

CBCT scans were used using the Carestream CS 8100 scanner (Carestream Dental LLC, Atlanta, Brazil), with the following settings: 90 kVp, 5 mA and exposure time of 8 seconds. Images were selected in DICOM (Digital Imaging and Communications in Medicine) format.

The DICOM images were opened in the *InVesalius* software version 3.1.0, a free software for visualization, processing and analysis of 3D medical images, widely used in Dentistry, where segmentation was used to select the enamel foci in the lesion. For this, the enamel mask available in the software was used, and the threshold values were adjusted to segment only pixels with intensity within the desired range. The segmented areas were measured in square millimeters (mm^2) and the spatial coordinates were recorded in relation to the anatomical reference of the lesion. Data were stored in electronic spreadsheets for statistical analysis.

Standardization of Hounsfield Units (HU)

The standardization of Hounsfield Units (HU) in CBCT scans is a fundamental element to ensure the reliability and consistency of measurements obtained in the images. Although HU values are typically used in conventional computed tomography and not adapted for CBCT due to differences in image acquisition and reconstruction processes, a rigorous calibration approach was adopted in this study to ensure HU standardization. A specially designed calibration

Rep Imagenol Dentomaxilofacial 2024 julio-diciembre; 3(2): 2024030202
e-ISSN: 2791-1888| 4 de 8
Disponible en: https://publicaciones.svrid.org.ve/index.php/rid

phantom containing reference materials with known densities was used, covering a wide range of HU values including soft tissues, bones, and dental enamel.

Calibration Phantom

Specially designed calibration phantom was used for this study. The phantom contained reference materials with known densities that covered a wide range of HU values, including densities representing soft tissues, bones, and dental enamel. Each material within the phantom was characterized by its specific HU value.

Calibration Procedure

The meticulous calibration procedure involved several specific steps. Before each image acquisition, the calibration phantom was positioned in the same location as the patients. Images of the phantom were acquired under the same exposure settings used for the patients. Subsequently, the CS 8100 tomograph underwent a specific calibration procedure, where images of the phantom were acquired under the same exposure settings used for patients.

Comparison and Adjustment

After acquiring the phantom images, the HU values measured in the regions of interest (ROI) corresponding to the reference materials within the phantom were compared with the known HU values. Any discrepancies were adjusted through a calibration correction procedure. This involved modifying the CBCT scan acquisition parameters, if necessary, to ensure that the HU values measured in the images accurately matched the reference values.

Continuous Verification

Before each new image acquisition session, the calibration procedure was repeated to ensure that the HU values remained consistent throughout the study. The standardization process ensures the reliability and consistency of HU measurements by using a calibration phantom with known densities and repeating the calibration procedure before each new image acquisition session. Challenges include variations in acquisition parameters and the influence of surrounding tissues, which were minimized through careful adjustments and continuous verification

This rigorous approach to HU standardization ensured that density values in the obtained images were reliable and independent of any variations in surrounding tissues or exposure parameters. In this way, we could guarantee the accuracy and validity of the measurements made during the study.

Statistical analysis

All data were organized and distributed in the Excel program (2019), and comparative analyses were performed using the SPSS Statistics software version 25.0 (IBM, Armonk, USA) and R (Statistical and graphical programming language, Lucent Technologies, Murray Hill, USA). Thus, to fulfill the research objectives, Kolmogorov-Smirnov tests were conducted to assess the normality of sample distribution, and for correlation between groups, the Pearson Product-Moment Test was employed, with a significance level set at 5% ($p < 0.05$).

RESULTS

Through the analysis of the DICOM images obtained in the *InVesalius* software, it was possible to identify hyperdense areas of enamel in the lesions (Figure 2). The Kolmogorov-Smirnov tests to assess the normality of sample distribution demonstrated that the means of the areas (p-value = 0.13) have a normal distribution (mean of 3.74 and SD + 0.38), and the average size (p-value = 0.02) has a normal distribution (mean of 2.54 and SD + 0.23). (Figure 3) (Figure 4).

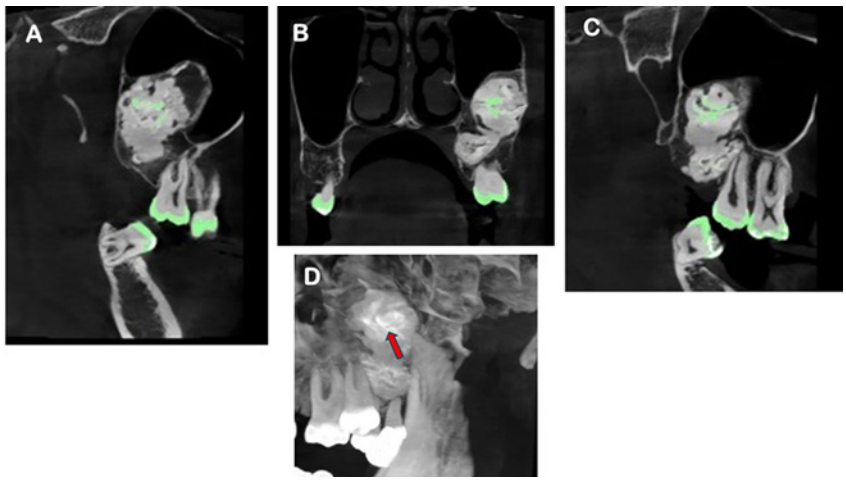

Figure 2. A, B, C: Sagittal and coronal tomographic slices and maximum intensity projection. In the sagittal and coronal tomographic sections, the areas colored green correspond to the applied enamel mask. D: Detected hyperdense foci. The arrow indicates areas of dental enamel in a complex odontoma.

Furthermore, the results of the Pearson Product-Moment Correlation to analyze whether there is a direct or indirect relationship between the mean and the average size demonstrated a statistically non-significant correlation (p-value = 0.67), indicating that the groups are independent and do not vary in a correlated manner. Therefore, it was possible to observe that the threshold image segmentation technique was effective in identifying areas of enamel in odontogenic lesions.

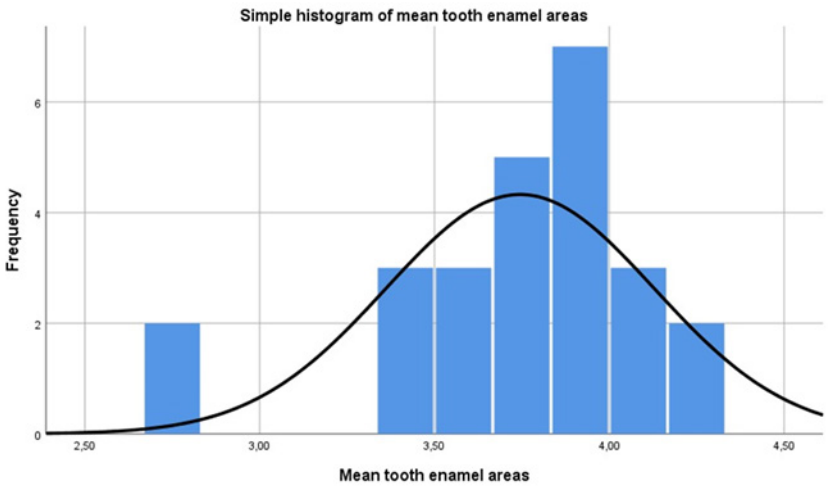

Figure 3. Kolmogorov-Smirnov test for enamel areas. The means of the areas (p-value = 0.13) have a normal distribution (Mean of 3.74 and SD+0.38).

Rep Imagenol Dentomaxilofacial 2024 julio-diciembre; 3(2): 2024030202
e-ISSN: 2791-1888| 6 de 8
Disponible en: https://publicaciones.svrid.org.ve/index.php/rid

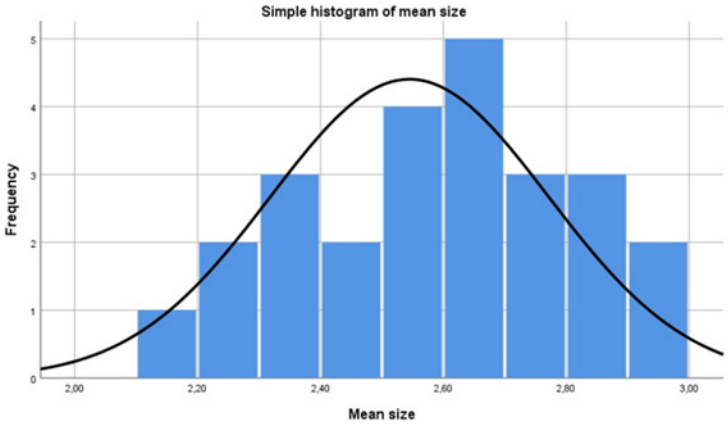

Figure 4. Kolmogorov-Smirnov test for mean tooth size. Average size (p-value = 0.02) has a normal distribution (Mean of 2.54 and SD + 0.23).

DISCUSSION

The use of advanced technologies in dentistry, such as CBCT, has been of great importance in the diagnosis and treatment of various injuries. However, the interpretation of the images obtained can be challenging, especially when dealing with lesions that have similar characteristics1,8. In this context, the InVesalius software, associated with the enamel mask, has proven to be an effective tool for detecting areas of enamel in odontogenic lesions, such as complex odontoma.The use of an enamel mask allowed a better visualization of the hyperdense areas in the CBCT images, facilitating the diagnosis and helping to identify lesions that present similar tomographic characteristics.

Several studies have highlighted the importance of CBCT in dental diagnostics and the challenges associated with image interpretation in complex cases. The use of segmentation software like InVesalius, coupled with enamel masks, provides a significant advantage in visualizing hyperdense regions. For instance, Lo Giudice et al. [7] demonstrated the accuracy of imaging software for 3D analysis of mandibular condyles, supporting our findings on the utility of InVesalius. Additionally, Kim [9] explored the potential of CBCT in assessing bone mineral density, which aligns with our efforts to standardize HU values for reliable measurements. These studies underscore the potential of InVesalius in routine evaluations for tomographic diagnosis, offering a reliable and cost-effective tool compared to other advanced imaging techniques.

The use of the *InVesalius* software for the detection of enamel areas in odontogenic lesions is possible thanks to the segmentation resource available in the program. This resource allows the selection of certain types of tissues present in the image, allowing the visualization of areas of enamel among other structures. For this, it is necessary to define a threshold that allows the selection of pixels with color intensity similar to that of enamel.

With the use of the enamel mask, it is also possible to isolate the selected areas in the original image, which facilitates their visualization and interpretation. This tool is especially useful in the differential diagnosis

of complex odontoma, which can be confused with other lesions that present hyperdense calcifications (Table 1) [14,16]. With the detection of areas of enamel in the lesions, it is possible to confirm the presence of odontogenic tissue and rule out other possible diagnostic hypotheses.

Table 1. Neoplasms of the orofacial complex that make differential diagnosis with odontoma.

LESIONS	RADIOLOGICAL CHARACTERISTICS
Cementoblastoma	Accumulation of cementoblasts in the periapical region of teeth; It presents as a well-delineated round radiopaque mass of disorganized cementum, surrounded by a radiolucent halo of germ cells.
Periapical cemento-osseous dysplasia	In a more advanced stage, it presents as a lesion with a dense nucleus and a radiopaque mineralized mass surrounded by a radiolucent zone.
Cemento-Ossifying Fibroma	Mass of fibrous and mineralized tissue of slow growth; It is presented as a radiopaque-radiolucent mixture. More advanced lesions become radiopaque due to progressive mineralization;
Condensing Osteitis	Focal area of well-circumscribed or ill-defined bony sclerosis around tooth roots
Idiopathic Osteosclerosis	Radiopaque area with sharp angular margins. Resembles a dense bone island
Dentinogenic Ghost Cell Tumor	Density mixed with the degree of calcification. They are typically well defined and may result in resorptions.
Adenomatoid Odontogenic Tumor	Characterization of mixed density with calcifications with the appearance of snow locos, usually with the presence of an impacted tooth
Calcifying Epithelial Odontogenic Tumor	It has varying densities from radiolucent to dense radiopaque. Its characteristic is that intralesional calcification is around a crown and is often associated with impaction of one or more teeth.

Source: Ghita et al.[14]; Vanhoenacker et al.[15]

The results obtained in this study showed an average of 3.8 enamel areas per complex odontoma lesion, with an average size of 2.5 mm². These values are consistent with data found in the literature, which suggests that the use of the enamel mask on the *InVesalius* can be a reliable tool for detecting areas of enamel in odontogenic lesions [16].

It is important to emphasize that the detection of areas of enamel in odontogenic lesions through the use of enamel mask should not be considered as a definitive diagnosis. It is necessary that the interpretation of the images be carried out by a qualified and experienced professional, who can evaluate all the clinical and tomographic aspects of the patient.

CONCLUSION

In conclusion, the use of the *InVesalius* software associated with the enamel mask proved to be an effective tool for detecting areas of enamel in odontogenic lesions, enabling the differential diagnosis of complex odontoma and other lesions that present hyperdense calcifications. However, the interpretation of the images must be carried out by a qualified professional, who considers all clinical and tomographic aspects of the patient.

Conflicts of Interest: The authors declare that they have no conflicts of interest.

Corresponding author:
Luana Leal. Afonso Pena Street, 1528, Pindorama. Faculty of Dentistry, Universidade Estadual de Piauí. Parnaíba, Brazil.
luanalccardoso@ outlook.com

Rep Imagenol Dentomaxilofacial 2024 julio-diciembre; 3(2): 2024030202
e-ISSN: 2791-1888| 8 de 8
Disponible en: https://publicaciones.svrid.org.ve/index.php/rid

REFERENCES

1. Nasseh I, Al-Rawi W. Cone beam computed tomography. Dent Clin North Am. 2018 Jul;62(3):361-91. DOI: https://doi.org/10.1016/j.cden.2018.03.002

2. Leonardi Dutra K, Haas L, Porporatti AL, Flores-Mir C, Nascimento Santos J, Mezzomo LA, Corrêa M, De Luca Canto G. Diagnostic accuracy of cone-beam computed tomography and conventional radiography on apical periodontitis: a systematic review and meta-analysis. J Endod. 2016 Mar;42(3):356-64. DOI: https://doi.org/10.1016/j.joen.2015.12.015

3. Ebert LC, Franckenberg S, Sieberth T, Schweitzer W, Thali M, Ford J, Decker S. A review of visualization techniques of post-mortem computed tomography data for forensic death investigations. Int J Legal Med. 2021 Sep;135(5):1855-67. DOI: https://doi.org/10.1007/s00414-021-02581-4

4. Wildberger JE, Prokop M. Hounsfield's Legacy. Invest Radiol. 2020 Sep;55(9):556-8. DOI: https://doi.org/10.1097/RLI.0000000000000680

5. Tsoumpas C, Sauer Jørgensen J, Kolbitsch C, Thielemans K. Synergistic tomographic image reconstruction: part 2. Philos Trans A Math Phys Eng Sci. 2021 Aug 23;379(2204):20210111. DOI: https://doi.org/10.1098/rsta.2021.0111

6. Centro de Tecnologia da Informação Renato Archer [Internet]. Software Inversalius: Guia do Usuário [Citado 18 de mayo de 2024]. Recuperado a partir de: https://www.gov.br/cti/pt-br/acesso-a-informacao/acoes-e-programas/invesalius

7. Lo Giudice A, Quinzi V, Ronsivalle V, Farronato M, Nicotra C, Indelicato F, Isola G. Evaluation of imaging software accuracy for 3-Dimensional analysis of the mandibular condyle. A comparative study using a surface-to-surface matching technique. Int J Environ Res Public Health. 2020 Jul 3;17(13):4789. DOI: https://doi.org/10.3390/ijerph17134789

8. Lo Giudice A, Ronsivalle V, Gastaldi G, Leonardi R. Assessment of the accuracy of imaging software for 3D rendering of the upper airway, usable in orthodontic and craniofacial clinical settings. Prog Orthod. 2022 Jun 13;23(1):22. DOI: https://doi.org/10.1186/s40510-022-00413-8

9. Kim DG. Can dental cone beam computed tomography assess bone mineral density? J Bone Metab. 2014 May;21(2):117-26. DOI: https://doi.org/10.11005/jbm.2014.21.2.117

10. Adibi S, Zhang W, Servos T, O'Neill PN. Cone beam computed tomography in dentistry: what dental educators and learners should know. J Dent Educ. 2012 Nov;76(11):1437-42.

11. Aldhuwayhi S, Bhardwaj A, Deeban YAM, Bhardwaj SS, Alammari RB, Alzunaydi A. A narrative review on current diagnostic imaging tools for dentomaxillofacial abnormalities in children. Children (Basel). 2022 Apr 27;9(5):621. DOI: https://doi.org/10.3390/children9050621

12. Silva BSF, Bueno MR, Yamamoto-Silva FP, Gomez RS, Peters OA, Estrela C. Differential diagnosis and clinical management of periapical radiopaque/hyperdense jaw lesions. Braz Oral Res. 2017 Jul 3;31:e52. DOI: https://doi.org/10.1590/1807-3107BOR-2017.vol31.0052

13. Araki M, Matsumoto N, Matsumoto K, Ohnishi M, Honda K, Komiyama K. Asymptomatic radiopaque lesions of the jaws: a radiographic study using cone-beam computed tomography. J Oral Sci. 2011 Dec;53(4):439-44. DOI: https://doi.org/10.2334/josnusd.53.439

14. Ghita I, Brooks JK, Bordener SL, Emmerling MR, Price JB, Younis RH. Central compact osteoma of the mandible: case report featuring unusual radiographic and computed tomographic presentations and brief literature review. J Stomatol Oral Maxillofac Surg. 2021 Nov;122(5):516-20. DOI: https://doi.org/10.1016/j.jormas.2020.09.014

15. Vanhoenacker FM, Bosmans F, Vanhoenacker C, Bernaerts A. Imaging of mixed and radiopaque jaw lesions. Semin Musculoskelet Radiol. 2020 Oct;24(5):558-569. DOI: https://doi.org/10.1055/s-0039-3402766

16. MacDonald-Jankowski DS. Odontomas in a Chinese population. Dentomaxillofac Radiol. 1996 Sep;25(4):186-92. DOI: https://doi.org/10.1259/dmfr.25.4.9084271. PMID: 9084271